



# NEW PHYSICS FROM THE FIRST DETECTION OF COHERENT ELASTIC NEUTRINO-NUCLEUS SCATTERING (CEvNS) WITH LIQUID ARGON

O. G. Miranda<sup>1</sup>, D.K. Papoulias<sup>2</sup>, G. Sanchez Garcia<sup>1</sup>, O. Sanders<sup>1</sup>, M. Tórtola<sup>3</sup> and J. W. F. Valle<sup>3</sup>.

<sup>1</sup>Departamento de Física, Centro de Investigación y de Estudios Avanzados del IPN, Mexico, <sup>2</sup>Division of Theoretical Physics, University of Ioannina, Greece, and <sup>3</sup>AHEP Group, Institut de Física Corpuscular – CSIC/Universitat de València, Valencia, Spain

## INTRODUCTION

The CENNS-10 experiment of the COHERENT collaboration has recently reported the first detection of coherent-elastic neutrino-nucleus scattering (CEvNS) on liquid Argon with more than  $3\sigma$  significance [1]. Through a dedicated statistical analysis of the new data, we derive a first measurement of the neutron rms charge radius of Argon, and also an improved determination of the weak mixing angle in the low energy regime. We also update the constraints on neutrino non-standard interactions, electromagnetic properties and light mediators with respect to those derived from the first COHERENT-CsI data.

## CEvNS IN THE STANDARD MODEL

Proposed more than forty years ago by Freedman [2], the neutral current CEvNS cross section scales as  $N^2$ , with  $N$  being the number of neutrons in the nucleus:

$$\left(\frac{d\sigma}{dT_A}\right)_{SM} = \frac{G_F^2 m_A}{2\pi} (Q_W^V)^2 \left[ 2 - \frac{2T_A}{E_\nu} - \frac{m_A T_A}{E_\nu^2} \right], \quad (1)$$

where  $G_F$  denotes the Fermi constant,  $T_A$  is the nucleus kinetic energy,  $E_\nu$  the neutrino energy and  $Q_W^V$  the vector weak charge written in the form:  $Q_W^V = [g_V^p Z F_p(Q^2) + g_V^n N F_n(Q^2)]$ . Here,  $Z$  and  $N$  are the number of protons and neutrons in the nucleus while the neutral current vector couplings,  $g_V^{p,n}$ , are given by:  $g_V^p = \frac{1}{2} - 2\sin^2\theta_W$ ,  $g_V^n = -\frac{1}{2}$ , with the weak mixing angle taken in the  $\overline{MS}$  scheme, i.e.  $\sin^2\theta_W \equiv \hat{s}_2^2 = 0.2312$ .

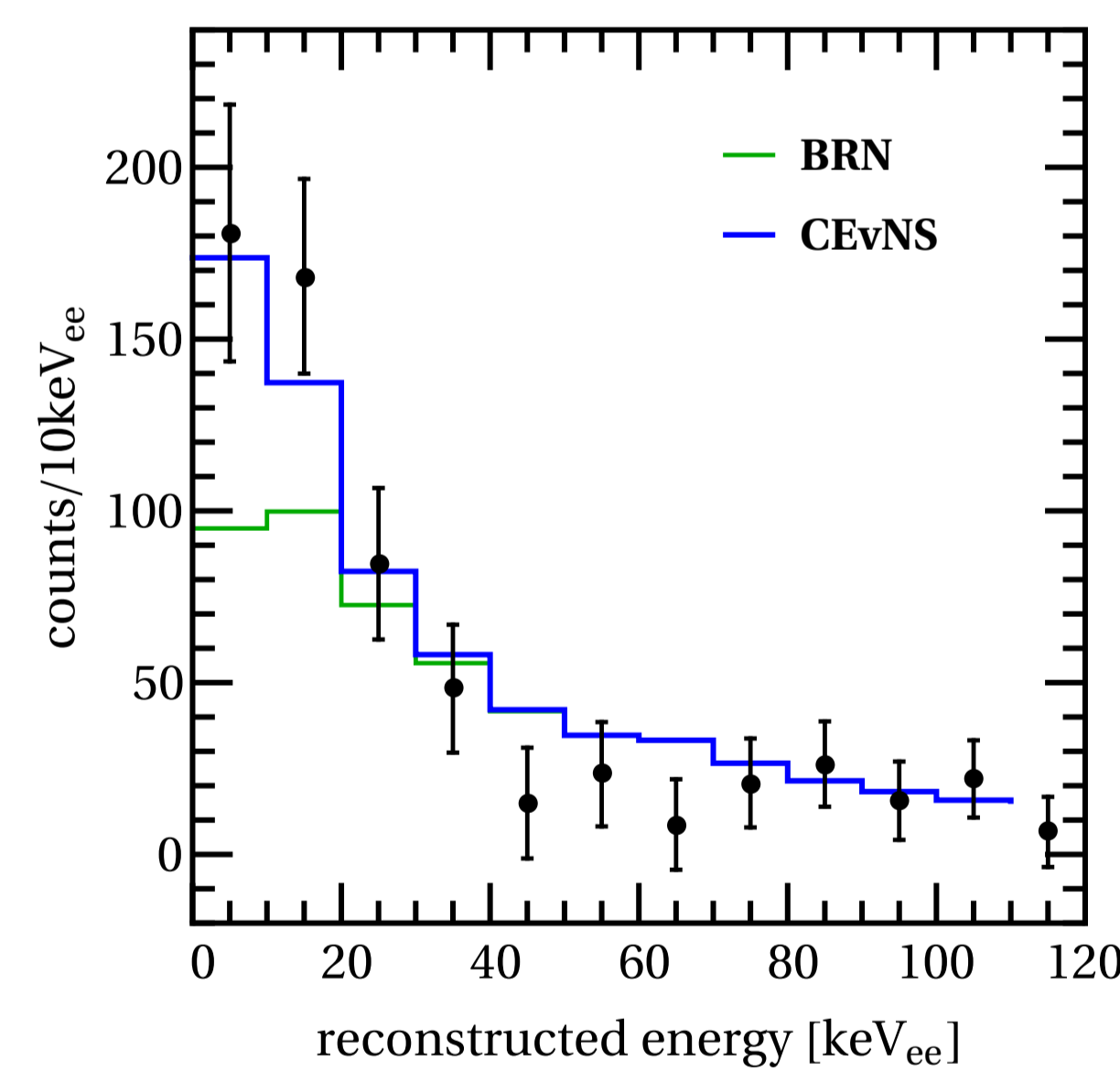
Finally,  $F_{p,n}(Q^2)$  stands for the nuclear form factors for protons and neutrons respectively, for which we employ the well-known Helm parametrization

$$F_{p,n}(Q^2) = 3 \frac{j_1(QR_0)}{QR_0} \exp(-Q^2 s^2/2), \quad (2)$$

where the magnitude of the three-momentum transfer is  $Q = \sqrt{2m_A T_A}$ , while  $j_1$  denotes the spherical Bessel function of order one and  $R_0^2 = \frac{5}{3}(R_{p,n}^2 - 3s^2)$  with  $R_n = 3.36$  fm ( $R_p = 3.14$  fm) denoting the neutron (proton) rms radius and  $s = 0.9$  fm.

FIGURE 1

COHERENT LAr



Simulated number of events at the CENNS-10 LAr detector as a function of the reconstructed electron recoil energy. The beam related neutron (BRN) and the experimental data are also shown [3].

The differential number of events is given by

$$\frac{dN_x}{dT_A} = \eta N_{\text{target}} \sum_{\nu_\alpha} \int_{\frac{m_A T_A}{2}}^{E_\nu^{\text{max}}} \mathcal{A}(T_A) \frac{d\phi_{\nu_\alpha}}{dE_\nu} \left(\frac{d\sigma}{dT_A}\right)_x dE_\nu, \quad (3)$$

where  $d\phi_{\nu_\alpha}/dE_\nu$  is the  $\pi$ -DAR neutrino spectrum,  $N_{\text{target}}$  is the number of nuclear targets in the CENNS-10 detector, and  $x = (\text{SM}, \text{new})$  denotes the type of interaction. Here,  $\eta$  denotes a normalization factor given by  $\eta = r N_{\text{POT}}/4\pi L^2$ , where  $L$  is the baseline,  $N_{\text{POT}}$  is the number of delivered POT,  $r$  is the number of produced neutrinos per POT and  $\mathcal{A}(T_A)$  is the detector efficiency.

## ACKNOWLEDGMENTS

The work of DKP is co-financed by Greece and the European Union (European Social Fund- ESF) through the Operational Programme «Human Resources Development, Education and Lifelong Learning» in the context of the project «Reinforcement of Postdoctoral Researchers - 2nd Cycle» (MIS-5033021), implemented by the State Scholarships Foundation (IKY).



## SM PRECISION TESTS

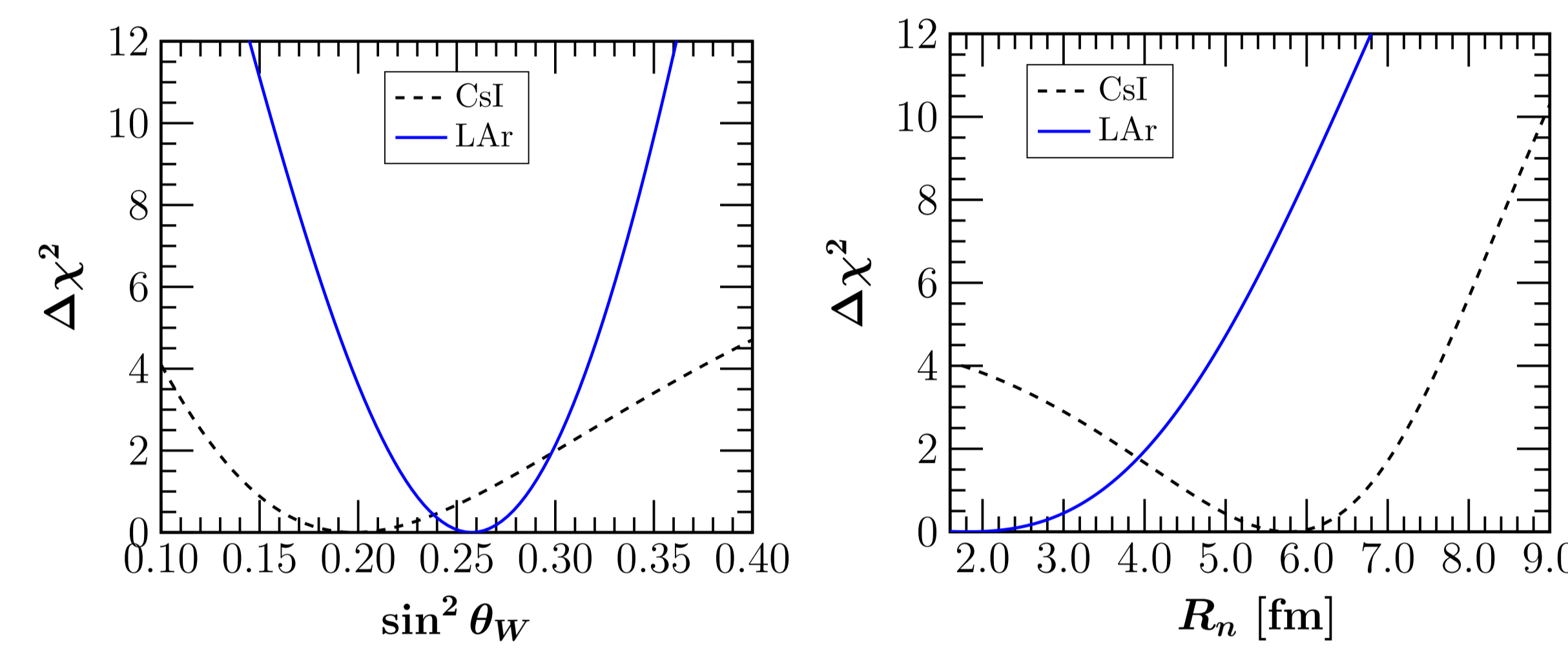
The weak mixing angle is measured with great accuracy at the  $Z$  peak. At low energies, however, the existing measurements are less precise but still very relevant given the prediction of an increase of about 3% in its value due to radiative corrections. The new measurement of the weak mixing angle, derived from the CENNS-10 data at 90% C.L. reads [3]

$$\sin^2\theta_W = 0.258_{-0.050}^{+0.048}. \quad (4)$$

Another very useful standard information that can be obtained from the CEvNS interaction is the neutron mean radius  $R_n$  for the Argon isotope, the determination of which can facilitate a better understanding of the CEvNS background at dark matter oriented experiments. Using CEvNS we obtained the first experimental determination of the neutron radius in Argon at 90% C.L. [3]

$$R_n < 4.33 \text{ fm}. \quad (5)$$

FIGURE 2



Sensitivity on the weak mixing angle (left) and on the neutron rms radius (right) [3]. A comparison between the results obtained with LAr and CsI detectors is also shown.

## ELECTROMAGNETIC NEUTRINO PROPERTIES

The non-vanishing neutrino mass implied by oscillation data points to the existence of non-trivial electromagnetic neutrino properties. Due to the helicity-violating nature of the neutrino magnetic moment cross section, there is no interference with the SM one given in Eq.(1) and yields an additive contribution of the form

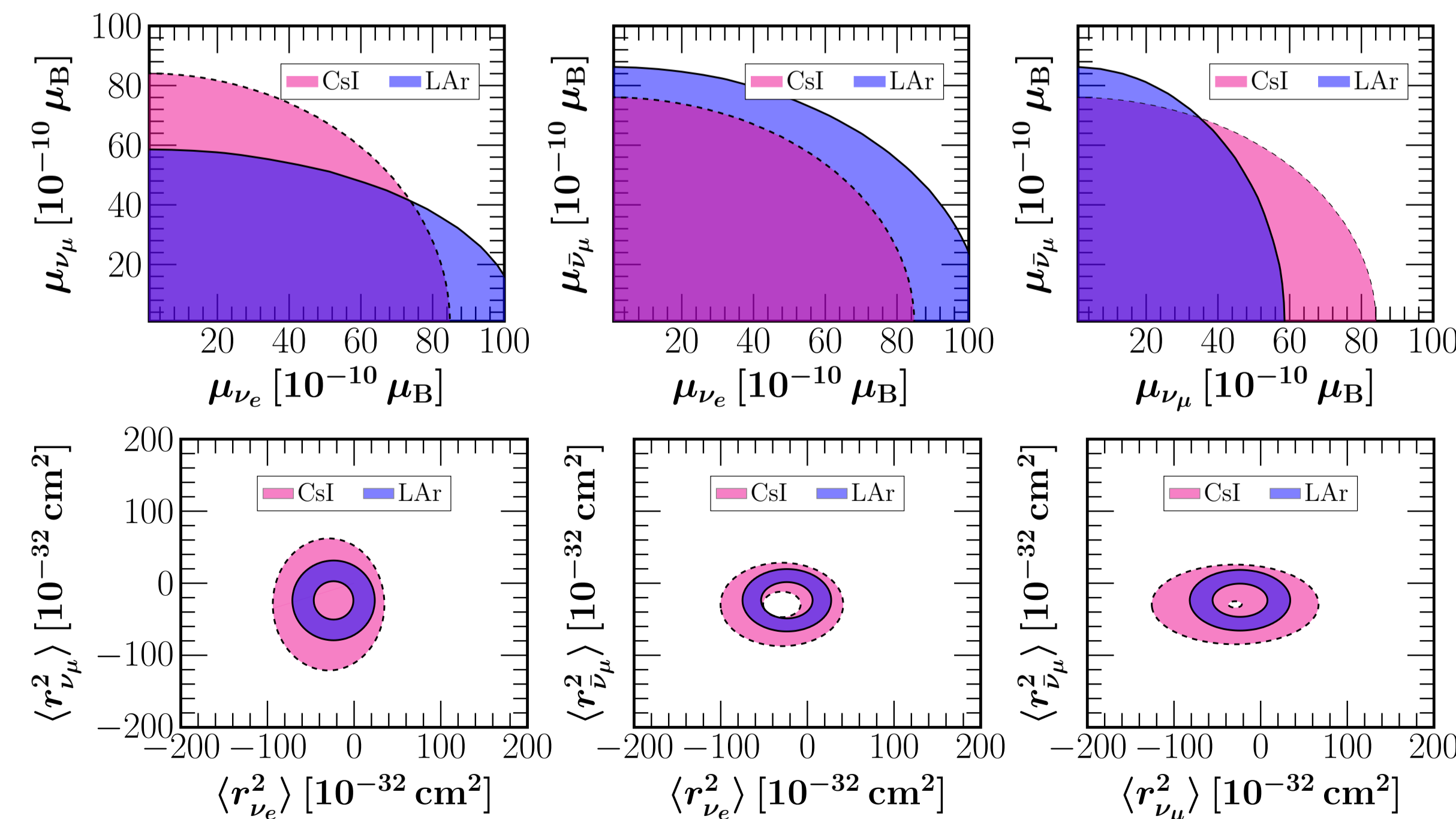
$$\left(\frac{d\sigma}{dT_A}\right)_{EM} = \frac{\pi \alpha_{EM}^2 \mu_\nu^2 Z^2}{m_\nu^2} \left(\frac{1 - T_A/E_\nu}{T_A}\right) F_p^2(Q^2). \quad (6)$$

Similarly, the impact of a non-zero neutrino charge radius to the SM cross section is simply taken as a shift on the weak mixing angle according to

$$\sin^2\theta_W \rightarrow \hat{s}_2^2 + \frac{\sqrt{2}\pi\alpha_{EM}\langle r_{\nu_\alpha}^2 \rangle}{3G_F}. \quad (7)$$

While the current constraints are not stringent, CEvNS provides a new window to probe  $\mu_{\nu_\mu}$  and  $\langle r_{\nu_\mu}^2 \rangle$

FIGURE 3



Upper panel: 90% C.L. allowed region in the parameter space of the neutrino magnetic moments ( $\mu_{\nu_\alpha}, \mu_{\nu_\beta}$ ). Lower panel: 90% C.L. allowed region in the parameter space of neutrino charge radii ( $\langle r_{\nu_\alpha}^2 \rangle, \langle r_{\nu_\beta}^2 \rangle$ ). The results are shown for different choices of neutrino flavours, with the undisplayed parameters in each case assumed to be vanishing [3]. For comparison, we show the results from the analysis of CsI and LAr data.

## NON STANDARD INTERACTIONS (NSIS)

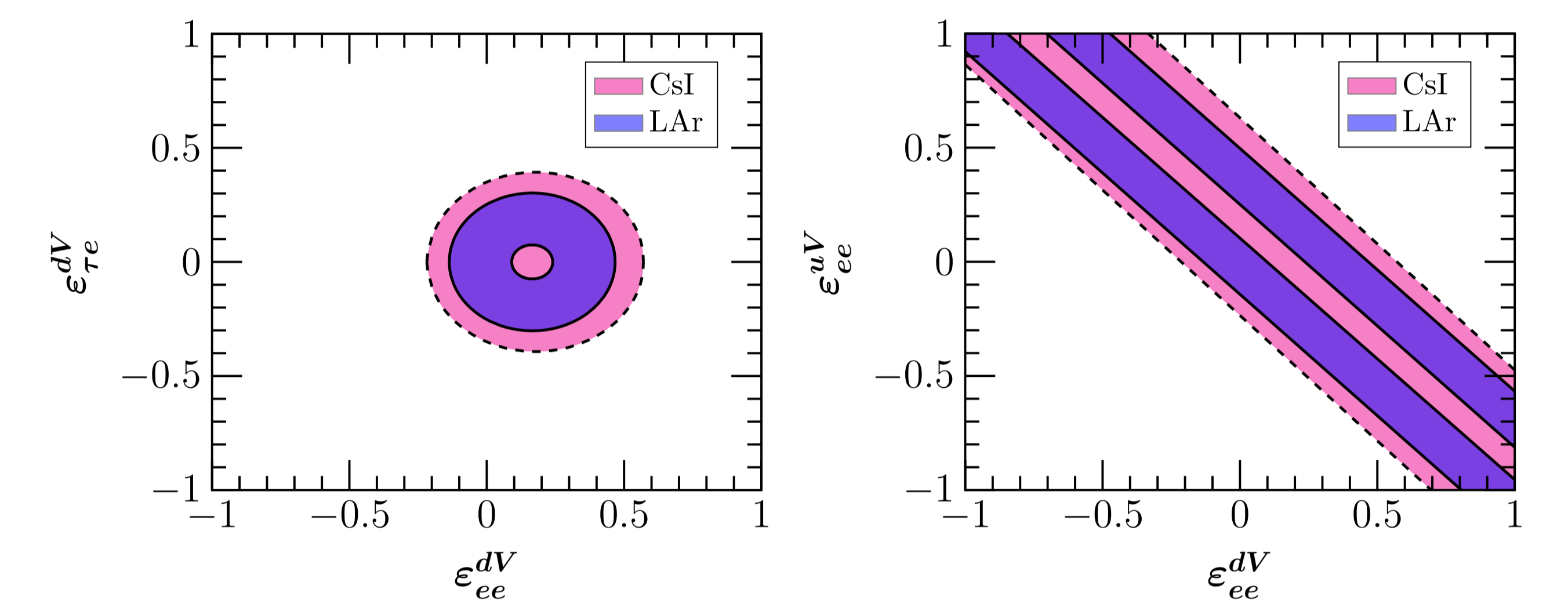
A large family of new physics models can be phenomenologically described using the formalism of NSI, that modify the neutral current SM Lagrangian through the contribution [4]

$$\mathcal{L}_{NC}^{NSI} = -2\sqrt{2}G_F \sum_{f,P,\alpha,\beta} \varepsilon_{\alpha\beta}^{fP} (\bar{\nu}_\alpha \gamma^\mu P_L \nu_\beta) (\bar{f} \gamma_\mu P_X f). \quad (8)$$

The weak charge of the CEvNS reaction is modified according to the substitution  $Q_W^V \rightarrow Q_{NSI}^V$  in Eq. (1), with the NSI charge given by

$$Q_{NSI}^V = \left[ (g_V^p + 2\varepsilon_{\alpha\alpha}^{pV} + \varepsilon_{\alpha\alpha}^{dV}) Z F_p(Q^2) + (g_V^n + \varepsilon_{\alpha\alpha}^{nV} + 2\varepsilon_{\alpha\alpha}^{dV}) N F_n(Q^2) \right] + \sum_\alpha \left[ (2\varepsilon_{\alpha\beta}^{uV} + \varepsilon_{\alpha\beta}^{dV}) Z F_p(Q^2) + (\varepsilon_{\alpha\beta}^{uV} + 2\varepsilon_{\alpha\beta}^{dV}) N F_n(Q^2) \right]. \quad (9)$$

FIGURE 4



90% C.L. allowed regions from the analysis allowing two NSI parameters at a time. The left panel considers the simultaneous presence of non-universal and flavor-changing NSI with  $d$  quark, while the right panel corresponds to the case of simultaneous non-universal NSI couplings with  $u$  and  $d$  quarks. A comparison is also given with the CsI data.

## LIGHT MEDIATORS

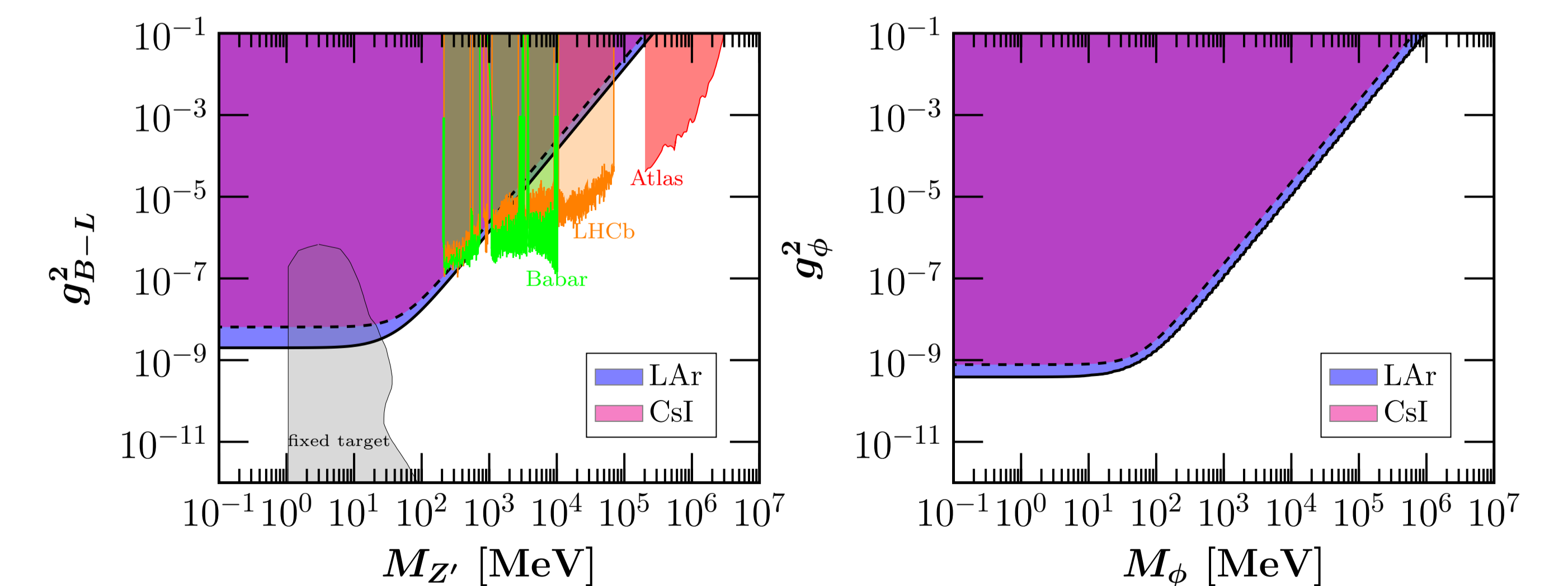
Simplified  $U(1)'$  scenarios with an additional vector  $Z'$  or a scalar  $\phi$  boson arise from [5]

$$\begin{aligned} \mathcal{L}_{\text{vector}} &= Z'_\mu (g_{Z'}^{qV} \bar{q} \gamma^\mu q + g_{Z'}^{lV} \bar{l} \gamma^\mu l), \\ \mathcal{L}_{\text{scalar}} &= \phi (g_\phi^{qS} \bar{q} q + g_\phi^{lS} \bar{l} l + \text{H.c.}), \end{aligned} \quad (10)$$

with  $M_{Z'}$  and  $M_\phi$  being the mass of the vector and scalar mediators, whereas  $g_{Z'}^{fV}$  and  $g_\phi^{fS}$  are the respective vector and scalar couplings to the fermion  $f = u, d, \nu$ .

CEvNS searches are clearly complementary, excluding a large part of the parameter space probed by ATLAS, beam-dump experiments, LHCb and BaBar.

FIGURE 5



Excluded region at 90% C.L. in the parameter space ( $M_{Z'}, g_{\beta-L}^2$ ) for the vector mediator scenario (left) and ( $M_\phi, g_\phi^2$ ) for the scalar mediator scenario (right), from the analysis of the recent LAr data [3]. A comparison is also given with the CsI data.

## References:

- [COHERENT Collaboration] D. Akimov et al., Phys.Rev.Lett. 126 (2021) 1, 012002.
- D.Z. Freedman, Phys.Rev.D 9 (1974) 1389-1392.
- O.G. Miranda, et al., JHEP 05 (2020) 130.
- O.G. Miranda, H. Nunokawa, New J.Phys. 17 (2015) 9, 095002.
- E. Bertuzzo et al., JHEP 04 (2017) 073.